Phycobilisome Mobility and Its Role in the Regulation of Light Harvesting in Red Algae[1][W]

Radek Kaňa*, Eva Kotabová, Martin Lukeš, Štěpán Papáček, Ctirad Matonoha, Lu-Ning Liu[2], Ondřej Prášil, and Conrad W. Mullineaux

Institute of Microbiology, Centre Algatech, Academy of Sciences of the Czech Republic, 379 81 Trebon, Czech Republic (R.K., E.K., M.L., O.P.); Faculty of Science, Institute of Chemistry and Biochemistry, University of South Bohemia, Branišovská 31, 370 05 Ceske Budejovice, Czech Republic (R.K., E.K., O.P.); Faculty of Fisheries and Protection of Waters, Center of Aquaculture and Biodiversity of Hydrocenoses, Institute of Complex Systems, University of South Bohemia in Ceske Budejovice, Zámek 136, 373 33 Nove Hrady, Czech Republic (Š.P.); Institute of Computer Science, Academy of Sciences of the Czech Republic, 18207 Praha 8, Czech Republic (C.M.); and School of Biological and Chemical Sciences, Queen Mary University of London, London E1 4NS, United Kingdom (L.-N.L., C.W.M.)

ORCID ID: 0000-0001-5768-6902 (R.K.).

Red algae represent an evolutionarily important group that gave rise to the whole red clade of photosynthetic organisms. They contain a unique combination of light-harvesting systems represented by a membrane-bound antenna and by phycobilisomes situated on thylakoid membrane surfaces. So far, very little has been revealed about the mobility of their phycobilisomes and the regulation of their light-harvesting system in general. Therefore, we carried out a detailed analysis of phycobilisome dynamics in several red alga strains and compared these results with the presence (or absence) of photoprotective mechanisms. Our data conclusively prove phycobilisome mobility in two model mesophilic red alga strains, *Porphyridium cruentum* and *Rhodella violacea*. In contrast, there was almost no phycobilisome mobility in the thermophilic red alga *Cyanidium caldarium* that was not caused by a decrease in lipid desaturation in this extremophile. Experimental data attributed this immobility to the strong phycobilisome-photosystem interaction that highly restricted phycobilisome movement. Variations in phycobilisome mobility reflect the different ways in which light-harvesting antennae can be regulated in mesophilic and thermophilic red algae. Fluorescence changes attributed in cyanobacteria to state transitions were observed only in mesophilic *P. cruentum* with mobile phycobilisomes, and they were absent in the extremophilic *C. caldarium* with immobile phycobilisomes. We suggest that state transitions have an important regulatory function in mesophilic red algae; however, in thermophilic red algae, this process is replaced by nonphotochemical quenching.

Photosynthetic light reactions are mediated by pigment-binding protein complexes located either inside the thylakoid membrane (e.g. chlorophyll-binding proteins of both photosystems) or associated on the membrane surface (e.g. phycobilisomes [PBsomes] in cyanobacteria and red algae). Recent progress in structural biology has allowed the construction of high-resolution structural models of most photosynthetic protein complexes (for review, see Fromme, 2008) together with their large-scale organization into supercomplexes (for review, see Dekker and Boekema, 2005). However, the dynamics of these supercomplexes and the mobility of particular light-harvesting proteins in vivo are still poorly understood (for review, see Mullineaux, 2008a; Kaňa, 2013; Kirchhoff, 2014) The importance of protein mobility in various photosynthetic processes, like nonphotochemical quenching and state transitions, has been explored mostly based on indirect in vitro experiments, including single-particle analysis (Kouřil et al., 2005), or by biochemical methods (Betterle et al., 2009; Caffarri et al., 2009). Recent studies on the mobility of light-harvesting proteins using live-cell imaging (for review, see Mullineaux, 2008a; Kaňa, 2013) have elucidated the importance of protein mobility for photosynthetic function (Joshua and Mullineaux, 2004; Joshua et al., 2005; Goral et al., 2010, 2012; Johnson et al., 2011). In addition, the redistribution of respiratory complexes in cyanobacterial thylakoid membranes plays an essential role in controlling electron flow (Liu et al., 2012).

[1] This work was supported by the Czech Science Foundation (grant no. GAČR P501–12–0304) and the Ministry of Education, Youth, and Sports of the Czech Republic (grant no. CZ.1.05/2.1.00/03.0110 to the Algatech Project), by a Marie Curie Fellowship from the European Commission (contract no. FP7–PEOPLE–2009–IEF 254575 to L.-N.L.), by the South Bohemian Research Center of Aquaculture and Biodiversity of Hydrocenoses CENAKVA (grant no. CZ.1.05/2.1.00/01.0024 to Š.P.), by the Ministry of Education, Youth, and Sport of the Czech Republic (National Sustainability Program I project no. LO1205 to Š.P.), and by the Institute of Computer Science (grant no. RVO:67985807 to C.W.M.).

[2] Present address: Department of Plant Sciences, Institute of Integrative Biology, University of Liverpool, Liverpool L69 7ZB, UK.

* Address correspondence to kana@alga.cz.

The author responsible for distribution of materials integral to the findings presented in this article in accordance with the policy described in the Instructions for Authors (www.plantphysiol.org) is: Radek Kaňa (kana@alga.cz).

[W] The online version of this article contains Web-only data.
www.plantphysiol.org/cgi/doi/10.1104/pp.114.236075

It is generally accepted that the mobility of most of the transmembrane photosynthetic proteins is very restricted in the thylakoid. The typical effective diffusion coefficient of photosynthetic proteins is somewhere between 0.01 and 0.001 $\mu m^{-2}\ s^{-1}$ (Kaňa, 2013). A similar restriction in membrane protein mobility has also been described for bacterial membranes (Dix and Verkman, 2008; Mika and Poolman, 2011). In fact, this is very different in comparison with what we know for other eukaryotic membranes (e.g. plasma membrane and endoplasmic reticulum), where membrane-protein diffusion can be faster by 1 or 2 orders of magnitude (Lippincott-Schwartz et al., 2001). Therefore, macromolecular crowding of proteins has been used to rationalize the restricted protein mobility in thylakoid membranes of chloroplasts (Kirchhoff, 2008a, 2008b). Indeed, atomic force microscopy studies have shown that there is a dense packing and interaction of complexes in the photosynthetic membranes (Liu et al., 2011). Therefore, the diffusion of photosynthetic proteins in the thylakoid membrane is rather slow, and it increases only in less crowded parts of thylakoids (Kirchhoff et al., 2013). The current model of photosynthetic protein mobility thus proposes the immobility of protein supercomplexes, such as PSII (Mullineaux et al., 1997; Kirchhoff, 2008b), with only a small mobile fraction of chlorophyll-binding proteins represented by external antennae of photosystems, including light harvesting complex of PSII in higher plants (Consoli et al., 2005; Kirchhoff et al., 2008) or iron stress-induced chlorophyll-binding protein A in cyanobacteria (Sarcina and Mullineaux, 2004).

The restricted mobility of internal membrane supercomplexes (photosystems) contrasts with the relatively mobile PBsomes (Mullineaux et al., 1997; Sarcina et al., 2001). PBsomes are sizeable biliprotein supercomplexes (5–10 MD) attached to the thylakoid membrane surface with dimensions of approximately 64 × 42 × 28 nm (length × width × height; Arteni et al., 2008; Liu et al., 2008a). PBsomes are composed of chromophore-bearing phycobiliproteins and colorless linker polypeptides (Adir, 2005; Liu et al., 2005). They serve as the main light-harvesting antennae in various species, including cyanobacteria, red algae, glaucocystophytes, and cryptophytes. Although a single PBsome is composed of hundreds of biliproteins, absorbed light energy is efficiently transferred toward a specific biliprotein that functions as a terminal energy emitter (Glazer, 1989). From there, energy can be transferred to either PSI or PSII and used in photosynthesis (Mullineaux et al., 1990; Mullineaux, 1992, 1994). In typical prokaryotic cyanobacteria and eukaryotic red algae, PBsomes are composed of two main parts: (1) allophycocyanin (APC) core proteins adjacent to the thylakoid membrane; and (2) peripheral rod proteins made from phycocyanin only or from a combination of phycocyanin together with phycoerythrin. Such complex and modular composition allows for different spectroscopic properties of PBsomes and thus their complementary absorption in the spectral region that is not covered by chlorophyll-binding proteins.

PBsome mobility has been studied only in a few types of cyanobacteria (for review, see Kaňa, 2013). PBsomes have been recognized as a mobile element with an effective diffusion coefficient of about 0.03 $\mu m^2\ s^{-1}$ for *Synechococcus* sp. PCC 7942 (Mullineaux et al., 1997; Sarcina et al., 2001). The effective diffusion coefficient value depends on lipid composition, temperature, and the size of the PBsome (Sarcina et al., 2001). The diffusion coefficient reflects PBsome mobility, but it is not affected singularly by physical diffusion processes, and the role of PBsome-photosystem interaction is an open question (Kaňa, 2013). PBsome mobility seems to be related to the requirement of light-induced PBsome redistribution during state transitions (Joshua and Mullineaux, 2004). The mechanism of state transitions in cyanobacteria is still rather questionable (for review, see Kirilovsky et al., 2014). As PSII seems to be immobile, it has been suggested that PBsomes interact with photosystems only transiently and that physical redistribution (diffusion) of PBsomes is crucial for the state transition (Mullineaux et al., 1997). The importance of such long-distance diffusions, however, should be tested experimentally in more detail (Kaňa, 2013), as an alternative theory of the state transition proposed only slight PBsome movement (shifting) between photosystems (McConnell et al., 2002). However, in both cases, PBsome mobility (i.e. the PBsome's ability to move) is required (Kaňa, 2013).

Red algae are the eukaryotic representatives of phototrophs containing PBsomes (Su et al., 2010). They represent the ancestor of photosynthetic microorganisms from the red clade of photosynthesis (Yoon et al., 2006; Wang et al., 2013), which includes various model organisms such as diatoms, chromerids, or dinoflagellates. Red algae contain a unique combination of antennae systems on their membrane surfaces, which are formed mostly by hemispherical PBsomes (Mimuro and Kikuchi, 2003; Arteni et al., 2008). Red algae also contain transmembrane light-harvesting antennae (Vanselow et al., 2009; Neilson and Durnford, 2010; Green, 2011) associated mostly with PSI (Wolfe et al., 1994). Therefore, red algae represent a functionally important eukaryotic model organism; however, few facts are known about the regulation of its light-harvesting efficiency, although it seems to be connected with photoprotection in the reaction center (Delphin et al., 1996, 1998; Krupnik et al., 2013). The presence of photoprotective NPQ in PBsomes of prokaryotic cyanobacteria has been conclusively proven (Kirilovsky et al., 2014); however, this mechanism seems to be missing in eukaryotic phycobiliproteins of cryptophytes (Kaňa et al., 2012b) and red algae. Moreover, the presence (or absence) of PBsome mobility has not been confirmed conclusively (Liu et al., 2009).

Therefore, we carried out a detailed study of PBsome mobility in red algal chloroplasts to determine the role of mobility in the regulation of light-harvesting efficiency. We found that red alga PBsomes are a mobile protein complex with effective diffusion coefficient between 2.7×10^{-3} and $13 \times 10^{-3}\ \mu m^{-2}\ s^{-1}$ in all studied mesophilic strains. It contrasted with PBsomes in extremophilic red algal strains (*Cyanidium caldarium*), where

PBsome mobility under physiological conditions was highly restricted (effective diffusion coefficient of approximately 0.6×10^{-3} μm^{-2} s^{-1}). The restriction of PBsome mobility in extremophilic *C. caldarium* was due to a tight interaction of PBsomes with both photosystems and not to changes in lipid desaturation, an effect typical for extremophiles. The PBsome-photosystem interaction was weakened for *C. caldarium* grown at suboptimal temperatures, resulting in a pronounced increase in PBsome mobility thanks to PBsome decoupling from the photosystem. This result shows that PBsome mobility in this strain is limited by the strength of the PBsome-photosystem interaction rather than by the restriction of diffusion by factors such as macromolecular crowding. Moreover, our study allows us to describe two different models of light-harvesting antenna regulation in red algae. In mesophilic strains (*Porphyridium cruentum* and *Rhodella violacea*), absorbed light is redistributed between photosystems in a process of state transition that requires PBsome mobility. On the contrary, in extremophilic *C. caldarium*, PBsome are strongly coupled to photosystems and excess light is dissipated by a process of nonphotochemical quenching, as has been described recently (Krupnik et al., 2013).

RESULTS

PBsome Diffusion in Red Algae: Fluorescence Recovery after Photobleaching Images

The mobility of red alga PBsomes was detected by the fluorescence recovery after photobleaching (FRAP) method, which allows direct measurement of photosynthetic protein mobility (for review, see Kaňa, 2013). A 633-nm laser was used to excite PBsomes, and their emission was measured above 665 nm. The recovery of the fluorescence signal during the FRAP measurements reflected mostly PBsome mobility and not the mobility of chlorophyll-binding proteins with an emission in this range (Supplemental Fig. S1) because (1) the 633-nm excitation induces chlorophyll emission through PBsomes attached to photosystems, so PBsome mobility is required to see fluorescence recovery after bleaching; and (2) there is almost no mobility of chlorophyll-binding proteins (Supplemental Fig. S2), so chlorophyll-binding proteins cannot participate in the fluorescence recovery seen in Figure 1. Figure 1 thus represents a typical FRAP image sequence showing PBsome mobility in *P. cruentum*. Images were made every 8 s before and after the application of high-intensity bleach. The prebleach image (top left in Fig. 1) shows a typical distribution of PBsome fluorescence in a single cell of *P. cruentum*. Application of high laser intensity across the *x* axis (red rectangle in Fig. 1) reduced PBsome fluorescence to about 40% of the initial value. The observed fluorescence recovery in the bleached zone (yellow circle in Fig. 1) showed PBsome mobility in this red alga.

The kinetics of recovery of the PBsome fluorescence shown in Figure 1 was further analyzed numerically (Fig. 2). We quantified fluorescence changes during FRAP measurements by pixel averaging in part of the bleached area (yellow circle in Fig. 1). The plot confirmed the recovery of PBsome fluorescence in the place

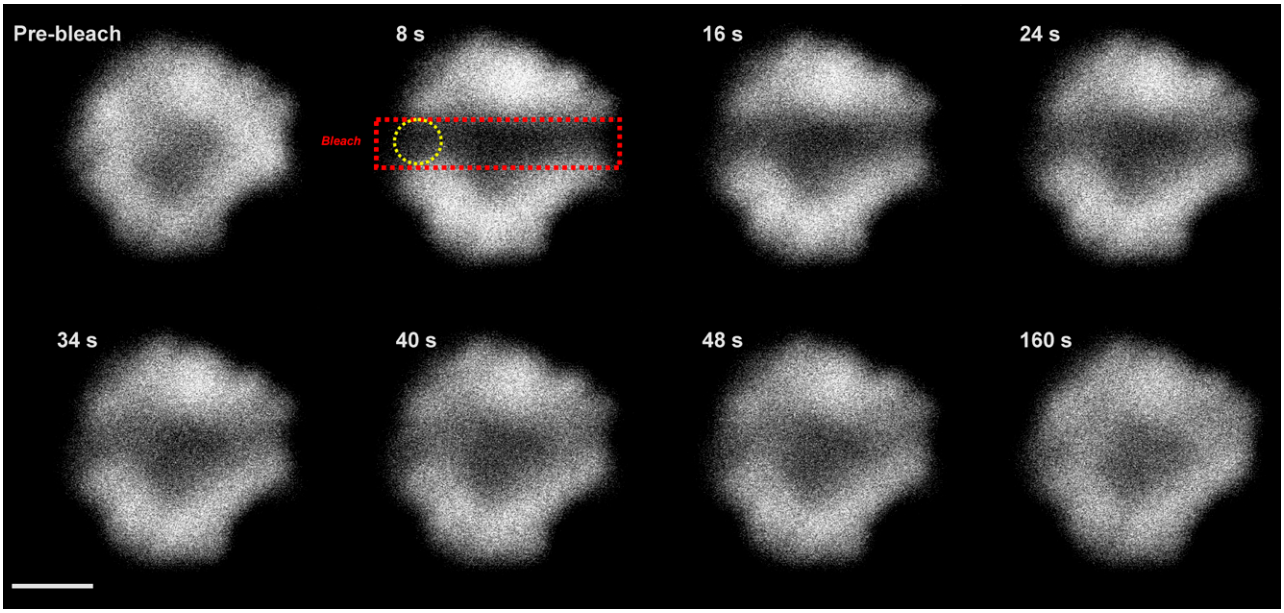

Figure 1. Representative FRAP image sequence for a single cell of *P. cruentum* for PBsome fluorescence. Fluorescence was excited at 633 nm, and emission was detected in the spectral range above 665 nm. First, a fluorescence image before bleaching was detected (Pre-bleach), and then the PBsome fluorescence was bleached out across the middle of the cell in the X direction (red rectangle); bleach depth (the extent of fluorescence decrease due to bleach application) was about 40% of the initial fluorescence intensity. Fluorescence in the middle of the membrane was used for further numerical analysis of the recovery in PBsome fluorescence (yellow circle). Time after bleaching is shown. Bar = 3 μm.

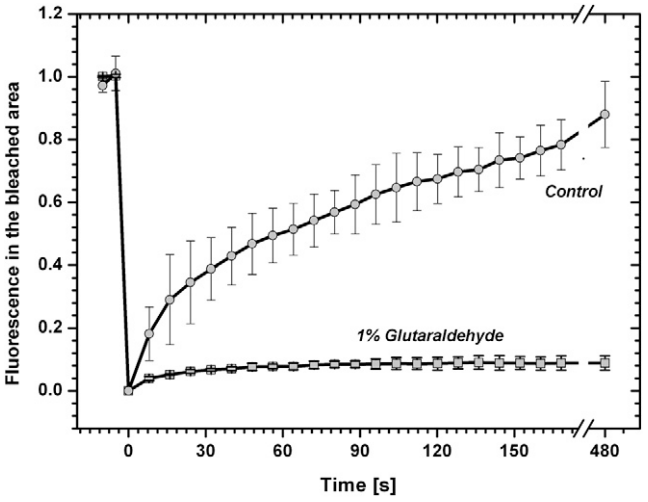

Figure 2. Time course of PBsome fluorescence recovery at the center of the bleached thylakoid of *P. cruentum*. The FRAP routine was measured for a control cell or with 1% glutaraldehyde, which cross links proteins and stops protein diffusion. Data were calculated from the FRAP image sequence presented in Figure 1; values are relative to fluorescence prior to bleaching, and the typical bleach depth before normalization was about 40% of the initial fluorescence. Data represent average values and SD for $n = 9$ with three biological replications.

of bleaching to about 80% of the initial value after 8 min of recovery. To exclude the possible effect of internal recovery in PBsome fluorescence due to the recovery of chromophore dark states (for review, see Kaňa, 2013), the FRAP routine was measured also for cells treated with 1% glutaraldehyde, which cross links proteins and stops protein mobility. In this case, we found only a very small recovery of fluorescence after bleaching (about 8%), which probably reflected the previously described internal fluorescence recovery in PBsomes (Liu et al., 2009). However, glutaraldehyde-insensitive recovery represented a dominant fraction of fluorescence recovery after photobleaching. Our data clearly show the presence of PBsome mobility and the minimal effect of internal fluorescence recovery in PBsomes of *P. cruentum*.

Properties of PBsome Diffusion in Red Algae

PBsome mobility was further studied by detailed analysis of bleach profiles (Fig. 3). The bleach profile represents a one-dimensional projection of fluorescence changes across the x axis in a selected area of the thylakoid (red rectangle in Fig. 3A and projection results in Fig. 3B), which can be used for the calculation of the effective diffusion coefficient (see "Materials and Methods"). Comparison of the prebleach and 8-s profiles (Fig. 3B) showed a decrease in PBsome fluorescence intensity (bleaching profile) due to the application of high-intensity laser power. The application of high-intensity bleach reduced total fluorescence to about 40% of the initial value due to the destruction of a portion of the phycobilin pigments (fluorescence intensity in the central bleached zone in Fig. 3A). The central zone was flanked by areas that showed a slight fluorescence increase immediately after bleaching (zone D, 1.5 μm, in Fig. 3, A and C). While the PBsome fluorescence in the central zone (central zone in Fig. 3A) slowly recovered with time after bleaching (16, 32, and 120 s in Fig. 3B), fluorescence intensity out of the bleached area (especially in zone D, 1.5 μm, in Fig. 3, A and C) was decreasing with time after bleaching. This loss of fluorescence out of the central zone (described as fluorescence loss in photobleaching; for review, see Kaňa, 2013) represents an additional proof of the diffusional exchange of nonfluorescent PBsomes from the central (bleached) zone with fluorescent PBsomes from the outer nonbleached zones. The exchange of fluorescent and nonfluorescent PBsomes is also visible in the detailed numerical analysis of fluorescence intensity in different distances from the middle of the bleached area (Fig. 3C). PBsome fluorescence in the central zone increased during the time-lapse experiment, in contrast with areas out of the central zone (1.5 and 1 μm in Fig. 3, A and C). Interestingly, at a distance of about 0.75 μm from the central zone, the movement of fluorescent PBsomes into and out of the 0.75-μm zone was equilibrated, resulting in a constant PBsome fluorescence during the whole time-lapse experiment (0.75 μm in Fig. 3C). These results provide a clear indication of PBsome mobility in *P. cruentum*.

Species Variability in PBsome Diffusion in Red Algae

We tested PBsome mobility in a mesophilic red alga with typical red algal hemispherical PBsomes, *P. cruentum* (Koller et al., 1977), and in *R. violacea*, which contains hemidiscoidal PBsomes that are more typical for cyanobacteria. The FRAP measurements proved that both of these types of PBsomes are mobile in mesophilic strains. Hemispherical PBsomes were significantly slower in their mobility (*P. cruentum* in Fig. 4) in comparison with much faster hemidiscoidal PBsomes (*R. violacea* in Fig. 4). In addition, the PBsome mobility was also measured in the extremophilic red alga *C. caldarium* (Fig. 4), which was isolated from highly acidic hot springs. Interestingly, PBsome mobility was almost undetectable (Fig. 4) in this extremophilic red alga grown at its optimal temperature at 38°C. Cultivation of *C. caldarium* at suboptimal temperatures (18°C) resulted in PBsome mobility (Fig. 4). However, this PBsome mobilization was accompanied by a very slow cell growth rate (Fig. 5), as the suboptimal temperature greatly increased doubling time. Therefore, the increase in PBsome mobility for *C. caldarium* from 18°C (Fig. 4) did not improve the vitality and physiology in these extremophilic red algae.

We further analyzed the extent of the PBsome mobile fraction in particular species. The steady-state value of fluorescence recovery at 480 s after bleaching was between 20% and 90% (Fig. 4). The internal effect of fluorescence recovery in PBsomes (diffusion-uncoupled fluorescence recovery; Kaňa, 2013) was estimated for all tested strains by FRAP measurements with

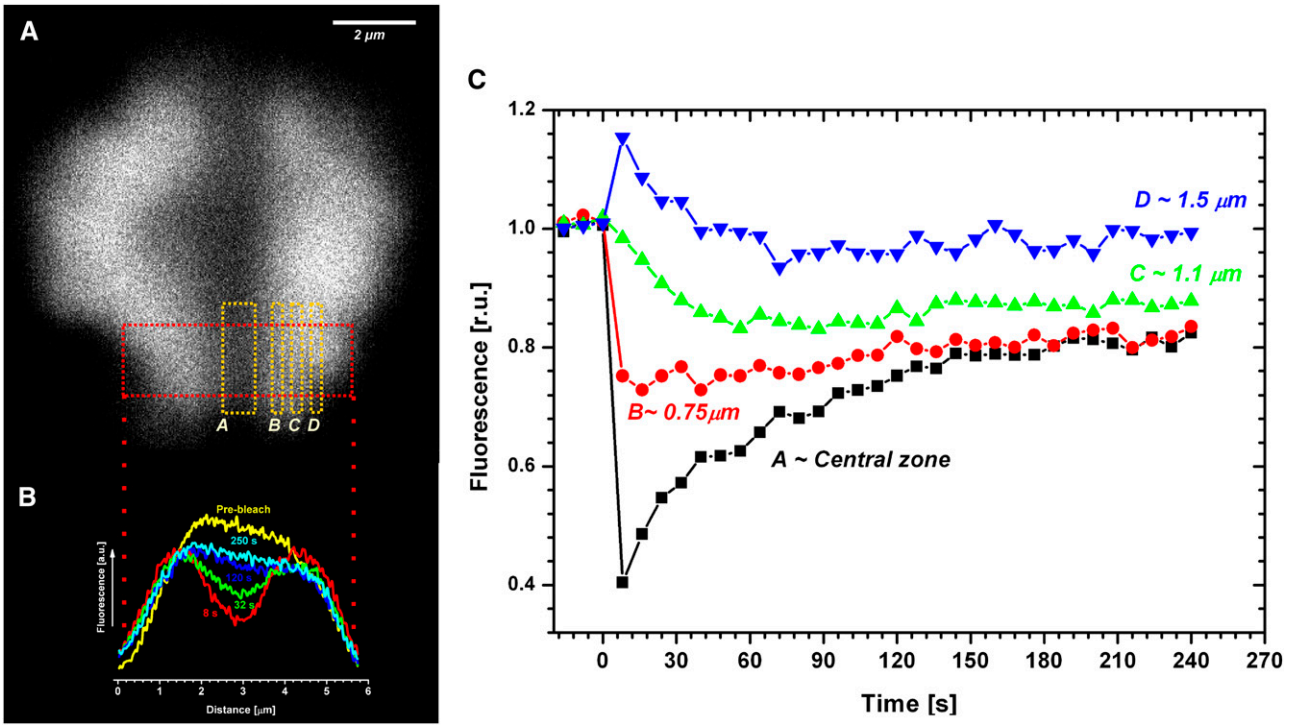

Figure 3. Detailed analysis of the bleach profiles during the measurement of PBsome mobility in the red alga *P. cruentum*. A, Representative image taken 8 s after bleaching. Areas (zones) with different distances from the central zone (A) are labeled by yellow rectangles as B (0.5 μm), C (1.1 μm), and D (1.5 μm). B, Typical dynamics of a one-dimensional bleach profile taken at characteristic times after bleaching (as labeled). Curves were constructed based on two-dimensional images at different time during the FRAP routine (Fig. 1) by averaging of two-dimensional data across *x* axes (the red curve 8 s represents averaging across the red rectangle in A). C, Dynamic changes in average values of the A to D zones presented in A during the FRAP routine (Fig. 1). r.u., Relative units.

1% glutaraldehyde, which can cross link proteins and stop protein diffusion (data not shown). Nevertheless, it represented only a minimal fraction of recovery, as in all tested strains it was below 10% (data not shown). The PBsome mobile fraction corrected for this internal effect is shown in Table I. Our analysis conclusively showed a relatively high mobile fraction of PBsomes in mesophilic red algae (79.2% and 88.9% for *P. cruentum* and *R. violacea*, respectively) and only a minimal mobile fraction of PBsomes in the extremophilic red alga *C. caldarium* (19.8%) at optimal growth conditions (38°C).

Effective diffusion coefficients of these mobile PBsomes were calculated numerically from the kinetics of bleach profiles (for details, see "Materials and Methods"). This analysis (Table I) showed significant variability in effective diffusion coefficients, with faster hemidiscoidal (*R. violacea*) and slower hemispherical (*P. cruentum*) PBsomes (between 2.7×10^{-3} and 13×10^{-3} $\mu m^{-2}\ s^{-1}$; Table I). It again confirmed the 10 times slower mobility of hemispherical PBsomes from red algae in comparison with hemidiscoidal PBsomes from the cyanobacterium *Synechococcus* sp. PCC 7942 (approximately 30×10^{-3} $\mu m^{-2}\ s^{-1}$; Mullineaux et al., 1997; Sarcina et al., 2001). It shows that hemispherical PBsomes have slower mobility in comparison with hemidiscoidal PBsomes.

In contrast with mesophilic species with diffusion coefficients between 2.7×10^{-3} and 13×10^{-3} $\mu m^{-2}\ s^{-1}$, PBsome mobility in the thermophilic *C. caldarium* grown at 38°C was 1 order of magnitude slower (around 0.57×10^{-3} $\mu m^{-2}\ s^{-1}$; Table I). We were able to stimulate PBsome diffusion in *C. caldarium* only by the cultivation of this strain at suboptimal temperatures (18°C), which had the effect of limiting growth rate (Fig. 5). In this case, PBsomes could move with a diffusion coefficient around 3.84×10^{-3} $\mu m^{-2}\ s^{-1}$ (Table I). We assume that the low diffusion coefficient value for PBsomes in *C. caldarium* grown at 38°C may be related to a stronger interaction of these PBsomes with photosystems, as there was only a minimal mobile fraction (Table I). This model has been tested by 77 K fluorescence spectroscopy (see below).

77 K Fluorescence Spectroscopy

Functional interaction was tested by means of 77 K fluorescence emission spectra by exciting PBsomes at 580 nm (Fig. 6). The 77 K fluorescence emission spectra showed typical bands (Fig. 6). We compared experimental spectra with the spectra detected from isolated protein complexes of both *P. cruentum* (Gantt et al.,

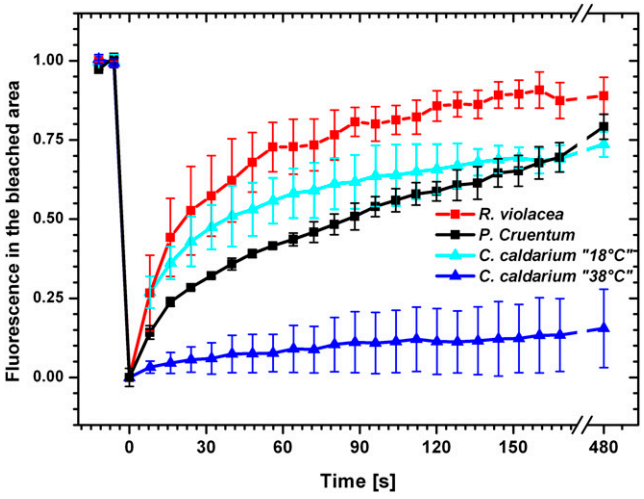

Figure 4. Time courses of fluorescence recovery for PBsome fluorescence in different red algae species, *P. cruentum*, *R. violacea*, and *C. caldarium*, grown at two temperatures, suboptimal 18°C (*C. caldarium* 18°C) and optimal 38°C (*C. caldarium* 38°C). Fluorescence values are relative to fluorescence prior to bleaching and were normalized to the changes in fluorescence in the nonbleached area. The effect of internal recovery was corrected by subtraction of FRAP curves measured with 1% glutaraldehyde (Fig. 2). Data represents averages and SD for $n = 12$.

1979; Bumba et al., 2004) and *C. caldarium* (Gardian et al., 2007; Busch et al., 2010). This allowed us to interpret the observed emission maxima as follows: (1) fluorescence emission at 644 nm in *P. cruentum* (F644 in Fig. 6A) was due to R-phycocyanin fluorescence emission (Ley et al., 1977), and emission at 650 nm in *C. caldarium* (F650 in Fig. 6B) originated from C-phycocyanin; (2) fluorescence emission around 661 nm (F661 in Fig. 6C) represented APC fluorescence; (3) fluorescence maxima around 684 nm (F684 in Fig. 6) represented a mixture of chlorophyll *a* fluorescence from PSII and APC-B emission of a terminal PBsome emitter (Ley et al., 1977); (4) fluorescence emission around 694 nm (F694, F695) is emitted from PSII; and (5) far-red light emission forms in *P. cruentum* (F708 in Fig. 6A) and in *C. caldarium* (F728 in Fig. 6B) reflected the fluorescence of red chlorophylls from PSI and its antennae. The 77 K fluorescence emission spectra for excitation of PBsomes (at 580 nm) were further used as a rough estimate of energy transfer from PBsomes to PSI (reflected by fluorescence emissions F708 and F728) or to PSII (reflected by F695 emission). The significant emission from both photosystems following excitation to PBsomes clearly showed PBsome energy flow to PSI and PSII.

We also studied the PBsome interaction with photosystems in *C. caldarium* grown at 18°C, which showed a higher mobile fraction of PBsomes (Table I). The F695-F728 ratio for excitation to PBsomes at 580 nm was the same for *C. caldarium* grown at 18°C and 38°C (Fig. 6C), so it did not change during adaptation to low temperature. The adaptation to the suboptimal temperature also did not affect the PSI-PSII ratio, as can be deduced from the F695-F728 ratio with excitation of chlorophylls at 434 nm, which was around 0.06 for *C. caldarium* from both growth temperatures of 38°C and 18°C (Fig. 6B). There was only a small decrease in the relative amount of PBsome in comparison with chlorophyll (compare PBsome absorbance at approximately 625 nm and chlorophyll at approximately 675 nm in Supplemental Fig. 3, A and B and Supplemental Table S1) between *C. caldarium* grown at 18°C and 38°C. The dominant change we observed during adaptation to low-temperature stimulation of PBsome mobility was a relative increase in PBsome fluorescence maxima between 650 and 684 nm (Fig. 6C), C-phycocyanin fluorescence (F650), and APC fluorescence (F662 and F684). Such an increase in PBsome fluorescence indicates a higher fraction of PBsomes that are energetically uncoupled from photosystems in *C. caldarium* grown at 18°C in comparison with cells grown at 38°C; we suggest that this is the reason for the higher mobile fraction of PBsomes in these cells (Table I). Therefore, the immobility of PBsomes in *C. caldarium* grown at 38°C is caused by a strong PBsome interaction with photosystems. As *C. caldarium* grew much faster at 38°C than at 18°C (Fig. 5), this indicates that the strong PBsome interaction with photosystems and the almost complete lack of PBsome mobility (Table I) represent an optimal physiological state in these thermophilic red alga allowing a faster growth rate. This contrasts with mesophilic red algae (*P. cruentum* and *R. violacea*), where PBsomes are present as fast mobile protein supercomplexes (Table I).

Composition of Lipids and PBsome Mobility

The interaction of PBsomes with photosystems is affected by lipid composition, especially by fatty acid saturation (Sarcina et al., 2001). Therefore, we quantified the extent of fatty acid saturation in two representatives

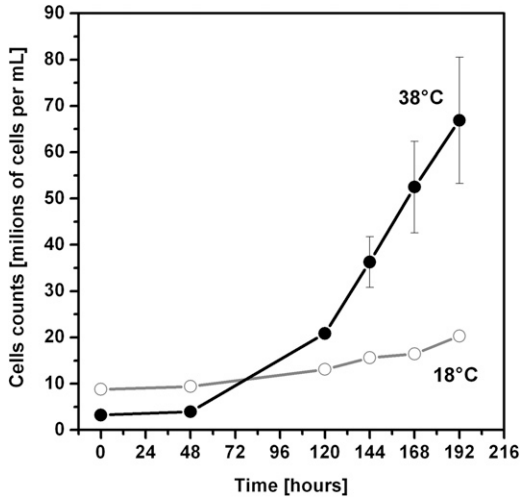

Figure 5. Growth curves of *C. caldarium* cells at 18°C or 38°C. Adapted cells from the stationary phase were diluted (to less than 10^7 cells mL^{-1}) and counted every 1 to 2 d by Multisizer 3.

Table I. *PBsome mobile fraction and effective diffusion coefficients*

Effective diffusion coefficient (D) was calculated from experimental FRAP data (see "Materials and Methods"). The presented mobile fraction represents fluorescence recovery 480 s after bleaching, where internal recovery of fluorescence unconnected with diffusion (recovery measured with glutaraldehyde) was subtracted. Data represent averages and SD for $n = 12$.

Parameter	*P. cruentum*	*R. violacea*	*C. caldarium* 38°C	*C. caldarium* 18°C
Mobile fraction (%)	79.2 ± 10.6	88.9 ± 5.7	19.8 ± 5.3	73.7 ± 7.8
D ($\times 10^{-3}$ μm^{-2} s^{-1})	2.69 ± 0.77	13.04 ± 9.15	0.57 ± 0.18	3.84 ± 2.19

red algae with mobile (*P. cruentum*) and immobile (*C. caldarium*) PBsomes grown at 18°C and 38°C. Isolated membranes of all three strains were analyzed by gas chromatography (see "Materials and Methods"). We detected typical fatty acids in various ratios (Table II). Four fatty acids (saturated C16:0 [palmitic acid] and C18:0 [stearic acid] and unsaturated C18:1n9 [oleic acid] and C18:2n6 [linoleic acid]) were detected in high amounts (above 1% from total lipid content) in all studied strains. There were few species-specific fatty acids (asterisks in Table II): highly unsaturated fatty acids detected only in *P. cruentum* (C18:3n6 [γ-linolenic acid], C20:4n6 [arachidonic acid], and C20:5n3 [eicosapentaenoic acid]) and fatty acids observed only in *C. caldarium* (C14:0 [myristic acid] and C18:3n3 [α-linolenic acid]). This indicates that mesophilic and thermophilic red algae adapt to different living conditions by changes in their membrane fatty acid composition; this is in line with previous studies done for *P. cruentum* (Khozin et al., 1997; Khozin-Goldberg et al., 2000) and *C. caldarium* (Allen et al., 1970).

The average extent of fatty acid unsaturation was characterized by the double bond index (DBI), which reflects membrane fluidity, as it represents a relative amount of double bonds in membrane lipids. The highest fatty acid saturation (lowest DBI) was observed in thermophilic *C. caldarium* cells with limited PBsome mobility; this is in line with the reduction in membrane fluidity (i.e. higher lipid saturation) usually observed during growth at higher temperatures. The low DBI observed in *C. caldarium* grown at 38°C increased only slightly during adaptation to low growth temperature (from 1.2 to 1.3; Table II). On the contrary, the membranes of the mesophilic red alga *P. cruentum* with mobile PBsomes (Table I) were more fluid, as shown by higher DBI (Table II). Therefore, higher PBsome mobility can be observed in more fluid membranes with more unsaturated lipids (i.e. with higher DBI). The effective diffusion coefficient and PBsome mobile fraction were higher (Table I) in more fluid membranes of mesophilic *P. cruentum* (higher DBI in Table II) and smaller in extremophilic *C. caldarium* grown at 38°C (Table I), which had less fluid membrane (lower DBI in Table II). However, the correlation between higher PBsome mobility and higher membrane fluidity was not general, as *C. caldarium* grown at 18°C had much higher PBsome mobility (Table I) without any significant increase in membrane fluidity based on DBI (Table II). There was also no change in the fatty acid chain length, another determinant for membrane fluidity, between *C. caldarium* cultures grown at 18°C and 38°C (Table II). Therefore, the stimulation of PBsome mobility in *C. caldarium* grown at 18°C in comparison with *C. caldarium* grown at 38°C is not caused by membrane fluidization due to lipid desaturation; rather, it is caused by a weakening of the photosystem-PBsome interaction,

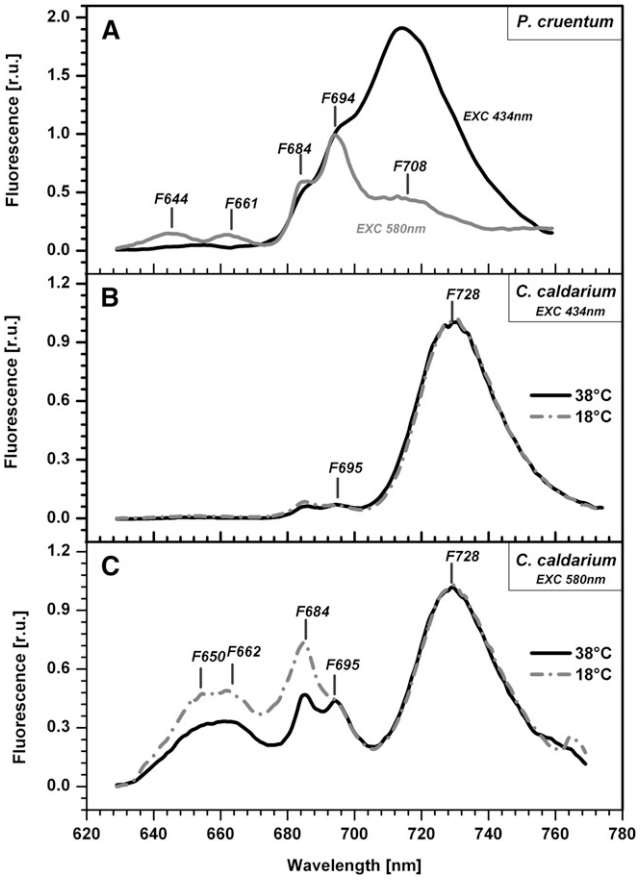

Figure 6. 77 K fluorescence emission spectra of *P. cruentum* and *C. caldarium*. A, 77 K fluorescence emission spectra of *P. cruentum* grown in optimal temperature (18°C) detected for excitation to PBsomes (at 580 nm; gray curve) or to chlorophyll *a* (at 434 nm; black curve). B, 77 K fluorescence emission spectra of *C. caldarium* grown in optimal (38°C) and suboptimal (18°C) temperatures that were detected for excitation to chlorophyll *a* (at 434 nm). C, 77 K fluorescence emission spectra of *C. caldarium* grown in optimal (38°C) and suboptimal (18°C) temperatures that were detected for excitation to PBsomes (at 580 nm). Data represent typical curves for dark-adapted cells normalized to 694 nm (A) or 728 nm (B and C). The positions of characteristic peaks are marked. r.u., Relative units.

Table II. *Fatty acid composition of red algae membranes*

Values represent DBI, average fatty acid chain length (FA chain), and relative amounts (in %) of the following fatty acids: C14:0, myristic acid; C16:0, palmitic acid; C16:1, palmitoleic acid; C18:0, stearic acid; C18:1n7, cis-7-octadecenoic acid; C18:1n9, oleic acid; C18:2n6, linoleic acid; C18:3n3, α-linolenic acid; C18:3n6, γ-linolenic acid; C20:3n6, dihomo-γ-linolenic acid; C20:4n6, arachidonic acid; and C20:5n3, eicosapentaenoic acid. Data represent average values and SD for $n = 3$. Asterisks indicate fatty acids that are specific either for extremophilic or mesophilic red algae. n.d., Not detectable.

Parameter	*P. cruentum*	*C. caldarium*	
		18°C	38°C
DBI	2.5 ± 0.2	1.3 ± 0.1	1.2 ± 0
FA chain	18.20 ± 0.05	17.47 ± 0.05	17.36 ± 0.01
C14:0	n.d.	0.40 ± 0.18*	0.26 ± 0.01*
C16:0	34.34 ± 0.94	26.69 ± 1.17	31.99 ± 0.15
C16:1	2.13 ± 0.36	0.46 ± 0.08	0.23 ± 0.07
C18:0	1.7 ± 0.8	4.77 ± 0.50	3.54 ± 0.25
C18:1n7	2.51 ± 1.53	0.55 ± 0.06	0.13 ± 0.03
C18:1n9	2.97 ± 2.5	6.43 ± 2.49	8.59 ± 0.04
C18:2n6	6.45 ± 0.72	58.89 ± 4.03	54.31 ± 0.55
C18:3n3	n.d.	0.56 ± 0.32*	0.18 ± 0.15*
C18:3n6	0.31 ± 0.05*	n.d.	n.d.
C20:3n6	0.55 ± 0.03	1.24 ± 0.18	0.78 ± 0.06
C20:4n6	16.24 ± 1.78*	n.d.	n.d.
C20:5n3	32.11 ± 3.41*	n.d.	n.d.

as indicated by the 77 K fluorescence spectra (Fig. 6). *C. caldarium* grown at suboptimal 18°C had a higher fraction of PBsomes uncoupled from photosystems (increase in PBsome fluorescence in Fig. 6C) that do not contribute to light harvesting.

Physiological Importance of PBsome Mobility

The presence of PBsome mobility in cyanobacteria has already been correlated with the occurrence of state transitions (Joshua and Mullineaux, 2004). It is a process that equilibrates absorbed energy distribution between photosystems (for review, see Kirilovsky et al., 2014). State transitions in cyanobacteria are typified by an increase in maximal fluorescence during the dark-light transition, as cyanobacteria are in the low-fluorescence state II in the dark. We observed a similar effect for dark-adapted *P. cruentum* exposed to low blue light but not in extremophile *C. caldarium* (Supplemental Fig. S4). This is, to our knowledge, the first indication showing the presence of state transitions in mesophilic red algae and its absence in extremophilic red algae. The process of state transition was further studied by the measurement of fluorescence changes in dark adapted cells during exposure to high orange light (Fig. 7). The fast light-induced fluorescence increase to its maximum (in hundreds of milliseconds) can be followed by another much slower fluorescence rise (in tens of seconds) from the plateau called S to the second M peak. Therefore, it is called the S-M rise. The S-M rise is dominant in cyanobacteria in contrast to the higher plants and green algae (for review, see Papageorgiou et al., 2007). The S-M rise was recently recognized as a result of the state 2-to-state 1 transition in cyanobacteria (Kaňa et al., 2012a). The slow fluorescence S-M rise in maximal fluorescence was detected also in *P. cruentum* between 10 and 50 s after irradiation of dark-adapted cells (Fig. 7A). The fluorescence increase was accelerated by the presence of 3-(3,4-dichlorophenyl)-1,1-dimethylurea, which amplified the state 2-to-state 1 transition due to a lack of plastoquinone pool reduction. On the contrary, the S-M fluorescence rise was fully stopped by 1% glutaraldehyde, which cross links proteins and also stops PBsome mobility measured from FRAP (Fig. 2). Therefore, we suggest that the presence of PBsome mobility in red algae correlates with state transition-induced changes in fluorescence in high-intensity orange light.

Indeed, the slow S-M fluorescence rise was totally missing in *C. caldarium* grown at optimal temperature (Fig. 7B), which also did not show any PBsome mobility. Moreover, there was no S-M fluorescence rise for *C. caldarium* from suboptimal growth temperatures (data not shown). This shows that an increase in PBsome mobility for *C. caldarium* grown at 18°C is not reflected in the appearance of state transitions. PBsomes in *C. caldarium* grown at 18°C are more weakly bound to photosystems, in contrast to *C. caldarium* grown in 38°C (compare the PBsome diffusion coefficient in Table I). The absence of the S-M rise in *C. caldarium* from 18°C also confirms that the higher PBsome diffusion coefficient observed at these conditions (3.84×10^{-3} μm^{-2} s^{-1}; Table I) is caused by a simple PBsome decoupling from photosystems and is not related to any physiological process of light energy

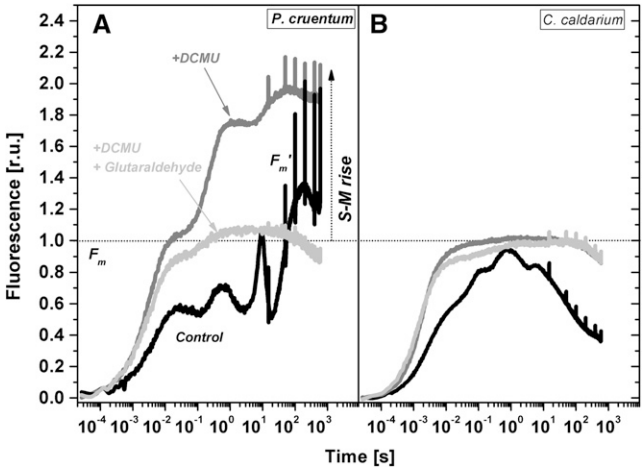

Figure 7. Time course of chlorophyll *a* fluorescence measured with *P. cruentum* (A) and *C. caldarium* (B). Samples without any addition (control) or in the presence (where indicated) of 10 μM 3-(3,4-dichlorophenyl)-1,1-dimethylurea (DCMU) or 1% glutaraldehyde are presented. Data are normalized to the maximal fluorescence obtained in the dark (F_m) before the fluorescence time course was recorded. Several saturation pulses were applied to obtain maximum fluorescence in the light (F_m'). The characteristic slow fluorescence rise (S-M rise) reflecting the state 2-to-state 1 transition is marked. For fluorescence excitation, orange diodes (λ_e = 590 nm, half-width $\Delta\lambda$ = ±20 nm) were used. r.u., Relative units.

distribution between photosystems. Therefore, PBsome mobility in *C. caldarium* is limited mostly by the strength of PBsome-photosystem interaction and not by a physical diffusion process. The state transition connected with PBsome redistribution, therefore, does not play such an important role in extremophilic red algae like *C. caldarium*. Rather, this species regulates energy arriving to PSII by some other mechanism, like nonphotochemical quenching in the reaction center of the extramophilic red alga *Cyanidioschyzon merolae* (Krupnik et al., 2013), or by excitation energy spillover between photosystems (Kowalczyk et al., 2013).

DISCUSSION

In this article, we show that PBsomes in mesophilic red algae are mobile light-harvesting antennae (Fig. 4), in line with PBsomes from prokaryotic cyanobacteria (for review, see Kaňa, 2013). By contrast, PBsomes in extremophilic red alga from hot acidic springs (*C. caldarium*) are almost immobile (Fig. 4; Table I), similar to the immobile phycobiliproteins in the lumen of cryptophytes (Kaňa et al., 2009b). The immobility of *C. caldarium* PBsomes is caused by their strong interaction with photosystems. This interaction is weaker in *C. caldarium* grown at suboptimal temperatures (18°C), resulting in PBsome decoupling from photosystems and a higher mobility (Fig. 4; Table I). Such PBsome decoupling from photosystems has been proposed to serve as one of the protoprotective mechanisms in cyanobacteria (Kaňa et al., 2009a; Tamary et al., 2012; for review, see Kirilovsky et al., 2014). In *C. caldarium*, PBsome decoupling from low growth temperature (18°C) causes increases in PBsome mobility measured by FRAP (Fig. 4; Table I). The increase in PBsome mobility was not accompanied by an increase in growth rate (Fig. 5), and it was also not involved in the stimulation of state transitions (Fig. 7). On the other hand, it could represent a photoprotective mechanism in extremophilic red algae to redirect excessive PBsome-absorbed irradiation away from the PBsomes (Kirilovsky et al., 2014).

We also observed a correlation between the presence of PBsome mobility and state transitions (measured from fluorescence) for PBsomes in mesophilic red algae (*P. cruentum*). In fact, the application of glutaraldehyde, cross linking PBsomes with photosystems, inhibits both processes, state transitions (Fig. 7) and PBsome mobility (Fig. 2). In comparison with cyanobacterial PBsomes in *Synechococcus* sp. PCC 7942 (Mullineaux et al., 1997), the effective diffusion coefficient for red algae PBsome has been found to be about 10 and three times less in *P. cruentum* and *R. violacea*, respectively (Table I). One possible explanation could be a different structure and organization of hemidiscoidal PBsomes in *Synechococcus* sp. PCC 7942 and hemispherical PBsomes from *P. cruentum*. In fact, PBsomes are represented by three distinct classes: (1) primitive rod-like PBsomes present in *Acaryochloris marina* (Theiss et al., 2011), in *Gloeobacter violaceus* (Krogmann et al., 2007), a common rock-dwelling organism (Mareš et al., 2013), and a similar rod-like PBsome with CpcG2 linker found in *Synechocystis* sp. PCC 6803 (Kondo et al., 2007); (2) widely distributed hemidiscoidal PBsomes are typical for cyanobacteria (e.g. *Synechococcus* sp. PCC 7942 and *Synechocystis* sp. PCC 6803) and for some red algae (e.g. *R. violacea*; Koller et al., 1977); and (3) hemispherical (hemiellipsoidal) types of PBsomes specific for most of the red algae, such as *P. cruentum* (Arteni et al., 2008). Our study demonstrates a reduced mobility of hemispherical PBsomes in comparison with hemidiscoidal ones (Fig. 4). However, the mobility of hemidiscoidal PBsomes in *R. violacea* is still slower in comparison with their analogs from *Synechococcus* sp. PCC 7942, with a diffusion coefficient of approximately $30 \times 10^{-3}\ \mu m^{-2}\ s^{-1}$ (Mullineaux et al., 1997; Sarcina et al., 2001). Therefore, PBsome mobility is not only affected by PBsome structure and size (Sarcina et al., 2001), and other factors also should be addressed in future experiments. The different PBsome mobilities in *P. cruentum* and *R. violacea* also could be caused by variations in the PBsome-photosystem ratio. To check this, we estimated the photosystem-PBsome ratio by means of deconvolution of absorption spectra (Supplemental Fig. S3; Supplemental Table S1). However, there was no significant difference in the photosystem-PBsome ratio (A_{440}/A_{630} in Supplemental Table S1), indicating that differences in this ratio are not the cause of the observed differences in PBsome mobility (Fig. 4). Indeed, the PBsome-photosystem ratio seems to be maintained constant over a wide range of growth conditions (Cunningham et al., 1989, 1990).

The slower PBsome mobility in red algae (in comparison with cyanobacteria) may be caused by PBsomes packing on thylakoid membrane surface, as reported recently for *P. cruentum* (Liu et al., 2008a). Such a crowded arrangement may seriously restrict PBsome diffusion due to the presence of physical obstacles, such as PBsomes (Liu et al., 2008a). This is similar to the effect that has already been found in the mobility of light-harvesting antennae in the overcrowded grana of higher plants (Kirchhoff, 2007). Another difference between cyanobacteria and red algae is the presence of intrinsic transmembrane light-harvesting antennae in red algae that are missing in cyanobacteria. It is plausible that the interaction of PBsomes with these antennae could slow PBsome mobility in red algae. The lower PBsome mobility in red algae in comparison with cyanobacteria could be the result of stronger PBsome-photosystem interaction, as the FRAP method reflects not only diffusional movement but also protein-protein interactions (Kaňa, 2013). The mobility of the relatively large PBsomes also could be affected by the limited width of the interthylakoidal space where the PBsome is situated. The flexibility of this interthylakoidal space might be another factor affecting changes in PBsome mobility. It was shown recently that the width of the interthylakoidal space can vary between light and dark (Nagy et al., 2012; Liberton et al., 2013). The importance of light-induced adjustment of the multilamellar thylakoid membrane system for the mobility of PBsomes and

other thylakoid proteins remains an open question that should be tested in future experiments.

Besides the mobile PBsomes, we also detected a small immobile fraction of PBsomes in mesophilic red algae (Table I). The immobile fraction was dominated in the extremophilic red alga *C. caldarium* under physiological conditions (*C. caldarium* 38°C in Fig. 4). The mobile fraction of PBsomes in *P. cruentum* (about 80%; Table I) was smaller in comparison with the cyanobacterium *Synechococcus* sp. PCC 7942, where roughly 100% of PBsomes are mobile (Mullineaux et al., 1997). This raises the question of the origin of this immobile fraction of PBsomes. This immobile fraction of PBsomes could be caused by the heterogeneity of the PBsome interaction with photosystems, as they act as an external antenna of both photosystems in cyanobacteria (Mullineaux, 1994; Ashby and Mullineaux, 1999; Rakhimberdieva et al., 2001) and also in red algae (Stadnichuk et al., 2011; Yokono et al., 2011). Moreover, there is a different organization of PSII in cyanobacteria (dimers) and red algae (tetrameric) in the arrangement of PSII complexes (Lange et al., 1990; Tsekos et al., 2004), which could explain the presence of an immobile fraction of PBsomes. The partial immobility of red alga PBsomes may be due to the presence of special proteins, called regulators of phycobilisome association with photosystems (the so-called Rpa-like proteins), that have already been described for cyanobacteria (Emlyn-Jones et al., 1999; Ashby et al., 2002; Joshua and Mullineaux, 2005). One of them, RpaC, a small transmembrane protein, has been recognized as a critical factor for state transitions, although its presence in red algae is questionable. Earlier biochemical studies suggested a role for one of the allophycocyan subunits, ApcE (sometimes called Lcm, for linker core membrane), in the PBsome-photosystem interaction (for review, see Liu et al., 2005; Mullineaux, 2008b). However, even though this protein is essential for the stabilization of the PBsome core, its direct role in PBsome binding to photosystems is still questionable (Ajlani and Vernotte, 1998).

The immobile PBsomes were dominant in the extremophilic red alga *C. caldarium*. Our data show the crucial role of the strength of the PBsome-photosystem interaction for the mobility/immobility of PBsomes in this organism. It has been suggested previously that the PBsome interaction with photosystems is rather weak and unstable; therefore, all PBsomes were considered to be uniformly mobile (Mullineaux et al., 1997; Sarcina et al., 2001). However, our results indicate that this assumption requires more direct experimental data in order to be confirmed. In the case of *C. caldarium*, the PBsome-photosystem interaction was weakened in *C. caldarium* grown at low temperatures (18°C) and was rather strong in *C. caldarium* grown at 38°C (Fig. 4; Table I). This has been deduced from the increase/decrease in PBsome fluorescence at 77 K, reflecting the lower/higher efficiency of energy transfer from PBsomes to photosystems (Fig. 6C). It resulted in the acceleration of the PBsome diffusion of *C. caldarium* from low temperatures and also in an increase of the mobile fraction of PBsomes from 20% to 74% (Table I). Since we have excluded the role of higher lipid desaturation in PBsome decoupling from photosystems (desaturation changed only slightly between 18°C and 38°C cultures of *C. caldarium*; Table II; Fig. 7), we suggest that the immobility of PBsomes in the extremophilic *C. caldarium* at optimal growth temperature is caused by a strong interaction of PBsomes with photosystems or with their antennae.

The firm interaction of PBsomes with PSI has been already shown in the extremophilic red alga *C. merolae*, a close relative *of C. caldarium*, where PSI together with membrane-extrinsic PBsome rods and integral membrane light-harvesting antennae form a very stable supercomplex (Busch et al., 2010). Moreover, such a tight coupling between antennae proteins in extremophilic red algae has already been found between PSI and its light-harvesting antennae (Thangaraj et al., 2011). This suggests that the stronger interaction between light-harvesting proteins in extremophilic red algae seems to be a consequence of their adaptation to high temperatures (above 40°C).

We also tried to determine the physiological importance of PBsome diffusion in red algae. In cyanobacteria, the presence of PBsome mobility has been correlated with the presence of state transitions (Joshua and Mullineaux, 2004) that act in the redistribution of absorbed light between PSI and PSII. Several mechanisms of state transitions have been suggested for cyanobacteria (for review, see Kirilovsky et al., 2014), and many of them propose PBsome displacement or at least slight PBsome rearrangement (McConnell et al., 2002; Joshua and Mullineaux, 2004; Kirilovsky et al., 2014). As photosystems and chlorophyll-binding proteins in cyanobacteria (Mullineaux et al., 1997) and in red algae (Supplemental Fig. S2) are almost immobile, the importance of PBsome mobility for the process of state transitions has already been suggested for cyanobacteria (Joshua and Mullineaux, 2004). Our data have revealed a similar correlation between PBsome mobility and state transitions in red algae. The correlation (between PBsome mobility and state transitions) does not necessarily mean the requirement of a long-distance PBsome diffusion for state changes. It only shows the necessity of some PBsome mobility for state changes. A limiting step for this mobility could be either a PBsome displacement (diffusion) or PBsome-photosystem interactions (Kaňa, 2013). The particular contribution and importance of those two processes need to be tested experimentally. These experiments are of special importance especially in light of the recent finding that PSI, PSII, and PBsomes can form a supercomplex (Liu et al., 2013) where PBsomes do not have to be moved far in order to induce a change in excitation flow from PBsomes to PSI or PSII.

It seems that in extremophilic red algae such as *C. caldarium*, state transitions are not so important in regulating light energy transfer between PBsomes and photosystems; the absence of state transitions correlates with the PBsome immobility in *C. caldarium* (Fig. 4). As a consequence, these extremophiles have developed other mechanisms to regulate energy arriving to reaction

centers: nonphotochemical quenching (fluorescence decrease in Fig. 7). Indeed, we recently conclusively proved the presence of a reaction center type of nonphotochemical quenching in the extremophilic red alga *C. merolae* (Krupnik et al., 2013).

All these results allow us to define two simplified models of light-harvesting antenna regulation in red algae with respect to PBsome (im)mobility. In the first mechanism, typical for mesophilic strains (*P. cruentum* and *R. violacea*), absorbed light can be redistributed between photosystems in a process of state transitions; therefore, PBsome mobility is relatively high. On the contrary, in extremophilic *C. caldarium*, PBsomes are strongly coupled to photosystems and excess light must be dissipated by a process on nonphotochemical quenching (Krupnik et al., 2013) or by PBsome decoupling (Liu et al. 2008b, Kirilovsky et al. 2014). An overlap between this model and other photoprotective mechanisms, like energy spillover between photosystems (Kowalczyk et al., 2013), is a matter for future research.

MATERIALS AND METHODS

Cell Growth and Sample Preparation

The mesophilic marine red alga *Porphyridium cruentum* (UTEX B637) was cultivated in adapted Porphyridium medium (Brody and Emerson, 1959), mesophilic *Rhodella violacea* was grown in an artificial seawater medium with f/2 nutrient addition (plus soil extract), and extremophilic *Cyanidium caldarium* was grown in Cyanidium medium, pH 2.5 (Allen, 1959). Low light intensity was used (approximately 30 μmol m^{-2} s^{-1}, with a day/night cycle of 12 h/12 h), and cells were continuously bubbled with air (Kaňa et al., 2012b). Temperature was set either to 18°C (*R. violacea* and *P. cruentum*) or 38°C (*C. caldarium*).

FRAP Measurements and Data Analysis

FRAP measurements of PBsomes were performed with a laser-scanning confocal microscope (Nikon PCM2000) equipped with a red helium-neon laser (633-nm line) and with a 60× oil-immersion lens of numerical aperture (NA) 1.4 and an Olympus FV1000 equipped with a red helium-neon laser (633-nm line) with a 100× oil-immersion UPLSAPO lens of NA 1.4 and a sampling speed 2 μs per pixel. The mobility of chlorophyll-binding proteins was measured with a laser-scanning confocal microscope (Nikon PCM2000) with a 60× oil-immersion lens of NA 1.4; fluorescence was excited by an argon laser (488 nm) and detected with a Schott RG665 red glass filter (transmitting above 665 nm). All measurements were performed at room temperature (20°C). A dichroic mirror transmitting above 650 nm (Nikon PCM2000) and a dichroic mirror with the edge at 635 nm (DM635; Olympus) were used to separate excitation and fluorescence light. The PBsome emission for measurements with the Nikon PCM2000 was selected with a Schott RG665 red glass filter (transmitting above 665 nm) and detected for a low laser power (approximately 3%). The PBsome emission for measurements with the Olympus FV1000 was selected using the variable bandpass filter system (100 nm above 655 nm).

The bleach line across the cell was induced with full red helium-neon laser power (for about 3 s) by fast switching the confocal microscope to X-scanning (Nikon PCM2000) or by the application of 100% intensity to a selected rectangular area of the cell (FV1000). The bleach intensity was set to reach about 40% bleach depth. Postbleach images were recorded typically every 8 s for 4 min with low laser power (10%). The series of FRAP images were analyzed with the Olympus FluorViewer 10-ASW software and with the public domain Java image-processing program ImageJ 1.45d (Abramoff et al., 2004). A one-dimensional bleaching profile was obtained by integration across the cell in the X direction in the parallel direction to the bleach line (Mullineaux et al., 1997). The baseline fluorescence from the unbleached cell was subtracted; the recovery curves were normalized to fluorescence changes in nonbleached cells, and double normalization including acquisition bleaching correction (Phair et al., 2004) was used during data processing.

Calculation of Effective Diffusion Coefficients from FRAP Results

Effective diffusion coefficients were calculated numerically based on a recently published method (Papáček et al., 2013). One-dimensional bleach profiles across x axes were constructed from experimental data exported from the FluorViewer 10-ASW software (Olympus) and further transformed in a two-dimensional data set using ImageJ 1.45d (Abramoff et al., 2004). A data set representing one-dimensional postbleach profiles was imported into the numerical software and used for effective diffusion coefficient calculation by a numerical routine without regularization (Papáček et al., 2013). The applied numerical algorithm is based on an algorithm that minimized the objective function representing differences between experimental data and numerical simulation. The numerical scheme was constructed based on the finite difference approximation of a one-dimensional Fickian diffusion equation. Dirichlet boundary conditions were applied for effective diffusion coefficient by numerical simulation of eight postbleach profiles.

The objective function was minimized for all eight postbleach profiles independently (Kaňa et al., 2013). The minimization of the objective function represents a one-dimensional optimization problem that was solved by the trust-region method from an open-source system of the universal functional optimization methods, a series of algorithms useful for solving optimization problems (Lukšan et al., 2013). The applied numerical routine (version FRAP 2.0) computed effective diffusion coefficients iteratively using the following parameters: (1) one-dimensional postbleach profiles were normalized to the same data taken from a prebleach image; (2) the first postbleach profiles were taken as initial conditions; (3) the central part of the bleach and surrounding areas were selected for analysis with an average size of around 2 μm; (4) data noise from all experimental data sets were reduced by smoothing using Fourier transformation; (5) the first eight postbleach profiles were used for numerical analysis; and (6) the Crank-Nicholson implicit scheme was used for the computation of simulated profiles (Papáček et al., 2013).

Lipid Extraction and Analysis

Cells were harvested at the exponential growth phase, collected biomass was centrifuged, and the pellet was diluted by resuspension in solution (800 μL of water, 2 mL of pure methanol, and 1 mL of dichloromethane [DCM]) and sonicated in an ultrasonic bath for 10 min at room temperature. The solution was diluted again in 1 mL of water and 1 mL of DCM and briefly vortexed. Phase separation of lipids in a glass tube with DCM was achieved by centrifugation (500*g*, 10 min, and 4°C), the lower DCM layer was removed and placed into clean evaporation vials with 2 mL of DCM, and the vortexing and centrifugation steps were repeated two more times. Lower phases were pooled and dried using a rotary evaporator. Dried extracts were redissolved in DCM:methanol (2:1, v/v) at a concentration of 1 mg of lipid extract per 20 μL and stored at –70°C for further analysis.

The lipid extract was methylated as described before (Kainz et al., 2002). An aliquot of lipid extract (approximately 0.5 mg) in DCM:methanol (2:1, v/v) was added to 15 μg of heptadecanoic acid and dried in a stream of N_2. The sample was diluted by mixing with 0.5 mL of hexane and 1 mL of 10% (w/w) borontrifluoride-methanol (Supelco, Sigma-Aldrich) and placed into a heating bath set to 85°C for 1 h. A total of 0.5 mL of chloroform-extracted water and 2 mL of hexane were added, and the sample was vortexed and centrifuged at 500*g* for 5 min. The upper hexane layer was removed to another vial for evaporation. The remaining mixture was washed two times with 2 mL of hexane as described above. Layers were pooled and concentrated under a stream of nitrogen to a final volume of 20 μL. Methylated samples (1 μL) were used for further quantitative and qualitative analysis on a GC-FID-HRGC 5300 device (Carlo Erba) equipped with a TR-FAME column (30 m × 0.32 mm, 0.25 μm film thickness; Thermo Fisher). Helium was used as the carrier gas at a pressure of 200 kPa. The temperature program was as follows: initial temperature of 140°C, temperature increase after injection at a rate of 4°C min^{-1} up to 240°C, and then constant temperature (240°C) for 10 min. The retention times of fatty acid methyl esters were compared with known standards (Supelco 37 Component FAME Mix and Supelco PUFA No. 3 [Supelco, Sigma-Aldrich]). Amounts of individual fatty acids were calculated as described before (Masood et al., 2005). The DBI was calculated as the sum of the relative contents of saturated fatty acids, each multiplied by the number of its double bonds. Fatty acid chain length was calculated as the sum of the relative contents of fatty acids, each multiplied by number of carbons in its fatty acid chain.

Fluorescence Measurements

Fluorescence emission spectra at 77 K for dark-adapted cells were measured with an Aminco-Bowman Series 2 spectrofluorometer (Thermo Electron). The sample was infiltrated on membrane filters that were fitted in a sample holder and immersed in an optical Dewar flask filled with liquid nitrogen. Possible effects of fluorescence reabsorption were tested for every sample by measuring spectra with different amounts of sample added to the filter and checking that the F695-F30 ratio was constant. Excitation was provided at 434 and 580 nm, each with a 4-nm bandwidth. Fluorescence emission was scanned with a 2-nm bandwidth between 630 and 800 nm. The experimental data were deconvoluted using Origin Pro 9.1 Peak Analyzer (OriginLab) using Gaussian curves. The positions of proposed peak maxima were restricted to a 4-nm range around the proposed maxima, and all other parameters were set to be free for the minimization procedure, driven by χ^2 (with 10^{-6} precision).

Chlorophyll *a* fluorescence induction kinetics were measured with the FL-100 Fluorometer (Photon Systems Instruments) as described previously (Kaňa et al., 2012a). Orange actinic light (590 nm; half-width $\Delta\lambda$ = 20 nm; 300 μmol m^{-2} s^{-1}) was used for excitation, and fluorescence induction was measured in the 690- to 750-nm range. Samples were dark adapted for 20 min before measurements, and the maximal fluorescence of closed PSII reaction centers was measured during a saturation flash (590 nm; length, 200 ms; approximately 1,200 μmol photons m^{-2} s^{-1}) in the dark. Subsequently, variable fluorescence kinetics, induced by orange actinic irradiation, were measured over a 10-min interval with logarithmically increasing intervals between the measured points. Fluorescence emission spectra were deconvoluted by Gaussian peaks in OriginPro version 9.1 (OriginLab) as described (Kaňa et al., 2009a).

Absorption Spectra

Absorption spectra were measured with a spectrophotometer (Unicam UV 550; Thermo Spectronic) equipped with an integrating sphere. Cells were collected on nitrocellulose membrane filters (Pragochema), and the filters were positioned in the integrating sphere. Absorbance was measured between 400 and 800 nm, with a bandwidth of 4 nm. Absorption spectra were deconvoluted by Gaussian peaks in OriginPro version 9.1 (OriginLab) as described (Kaňa et al., 2009a).

Physiological Measurements

The growth rate of *C. caldarium* was estimated using cell counts. For the estimation of growth rate at different temperatures, *C. caldarium* cells were adapted for 3 weeks to a given temperature (18°C or 38°C) before measurements. The adapted cells from the stationary phase were diluted (to less than 10^7 cells mL^{-1}) and counted every 1 to 2 d using a Multisizer 3 (Beckmann Coulter) with a 50-μm aperture in Isotone II (Beckmann Coulter).

Supplemental Data

The following materials are available in the online version of this article.

Supplemental Figure S1. Room temperature fluorescence emission spectra of the red alga strain *P. cruentum* for excitation to PBsomes at 615 nm.

Supplemental Figure S2. Mobility of chlorophyll-binding proteins of *P. cruentum*.

Supplemental Figure S3. Absorption spectra of *C. caldarium*, *P. cruentum*, and *R. violacea*.

Supplemental Figure S4. Changes in variable fluorescence in dark-adapted cells of *P. cruentum* and *C. caldarium* exposed to low blue light.

Supplemental Table S1. Results of the deconvolution of absorbance spectra presented in Supplemental Figure S3, with focus on chlorophyll (CHL − A_{440nm}) and phycocyanin + allophycocyanin (PC+APC − A_{630nm}) bands.

ACKNOWLEDGMENTS

We thank Jaroslav Krafl for carrying out additional FRAP experiments and data analysis, Jason Dean for reading the article, and Eva Žišková for the preparation of figures and graphic icon.

Received January 22, 2014; accepted June 17, 2014; published June 19, 2014.

LITERATURE CITED

Abramoff MD, Magelhaes PJ, Ram SJ (2004) Image processing with ImageJ. Biophotonics International **11:** 36–42

Adir N (2005) Elucidation of the molecular structures of components of the phycobilisome: reconstructing a giant. Photosynth Res **85:** 15–32

Ajlani G, Vernotte C (1998) Deletion of the PB-loop in the L(CM) subunit does not affect phycobilisome assembly or energy transfer functions in the cyanobacterium Synechocystis sp. PCC6714. Eur J Biochem **257:** 154–159

Allen CF, Good P, Holton RW (1970) Lipid composition of *Cyanidium*. Plant Physiol **46:** 748–751

Allen MB (1959) Studies with *Cyanidium caldarium*, an anomalously pigmented chlorophyte. Arch Mikrobiol **32:** 270–277

Arteni AA, Liu LN, Aartsma TJ, Zhang YZ, Zhou BC, Boekema EJ (2008) Structure and organization of phycobilisomes on membranes of the red alga Porphyridium cruentum. Photosynth Res **95:** 169–174

Ashby MK, Houmard J, Mullineaux CW (2002) The ycf27 genes from cyanobacteria and eukaryotic algae: distribution and implications for chloroplast evolution. FEMS Microbiol Lett **214:** 25–30

Ashby MK, Mullineaux CW (1999) The role of ApcD and ApcF in energy transfer from phycobilisomes to PSI and PSII in a cyanobacterium. Photosynth Res **61:** 169–179

Betterle N, Ballottari M, Zorzan S, de Bianchi S, Cazzaniga S, Dall'osto L, Morosinotto T, Bassi R (2009) Light-induced dissociation of an antenna hetero-oligomer is needed for non-photochemical quenching induction. J Biol Chem **284:** 15255–15266

Brody M, Emerson R (1959) The quantum yield of photosynthesis in Porphyridium cruentum, and the role of chlorophyll a in the photosynthesis of red algae. J Gen Physiol **43:** 251–264

Bumba L, Havelková-Dousová H, Husák M, Vácha F (2004) Structural characterization of photosystem II complex from red alga Porphyridium cruentum retaining extrinsic subunits of the oxygen-evolving complex. Eur J Biochem **271:** 2967–2975

Busch A, Nield J, Hippler M (2010) The composition and structure of photosystem I-associated antenna from Cyanidioschyzon merolae. Plant J **62:** 886–897

Caffarri S, Kouril R, Kereïche S, Boekema EJ, Croce R (2009) Functional architecture of higher plant photosystem II supercomplexes. EMBO J **28:** 3052–3063

Consoli E, Croce R, Dunlap DD, Finzi L (2005) Diffusion of light-harvesting complex II in the thylakoid membranes. EMBO Rep **6:** 782–786

Cunningham FX, Dennenberg RJ, Jursinic PA, Gantt E (1990) Growth under red light enhances photosystem II relative to photosystem I and phycobilisomes in the red alga *Porphyridium cruentum*. Plant Physiol **93:** 888–895

Cunningham FX, Dennenberg RJ, Mustardy L, Jursinic PA, Gantt E (1989) Stoichiometry of photosystem I, photosystem II, and phycobilisomes in the red alga *Porphyridium cruentum* as a function of growth irradiance. Plant Physiol **91:** 1179–1187

Dekker JP, Boekema EJ (2005) Supramolecular organization of thylakoid membrane proteins in green plants. Biochim Biophys Acta **1706:** 12–39

Delphin E, Duval JC, Etienne AL, Kirilovsky D (1996) State transitions or delta pH-dependent quenching of photosystem II fluorescence in red algae. Biochemistry **35:** 9435–9445

Delphin E, Duval JC, Etienne AL, Kirilovsky D (1998) ΔpH-dependent photosystem II fluorescence quenching induced by saturating, multiturnover pulses in red algae. Plant Physiol **118:** 103–113

Dix JA, Verkman AS (2008) Crowding effects on diffusion in solutions and cells. Annu Rev Biophys **37:** 247–263

Emlyn-Jones D, Ashby MK, Mullineaux CW (1999) A gene required for the regulation of photosynthetic light harvesting in the cyanobacterium Synechocystis 6803. Mol Microbiol **33:** 1050–1058

Fromme P, editor (2008) Photosynthetic Protein Complexes: A Structural Approach. Wiley-VCH, Weinheim, Germany

Gantt E, Lipschultz CA, Grabowski J, Zimmerman BK (1979) Phycobilisomes from blue-green and red algae: isolation criteria and dissociation characteristics. Plant Physiol **63:** 615–620

Gardian Z, Bumba L, Schrofel A, Herbstova M, Nebesarova J, Vacha F (2007) Organisation of photosystem I and photosystem II in red alga Cyanidium caldarium: encounter of cyanobacterial and higher plant concepts. Biochim Biophys Acta **1767:** 725–731

Glazer AN (1989) Light guides: directional energy transfer in a photosynthetic antenna. J Biol Chem **264:** 1–4

Goral TK, Johnson MP, Brain APR, Kirchhoff H, Ruban AV, Mullineaux CW (2010) Visualizing the mobility and distribution of chlorophyll proteins in higher plant thylakoid membranes: effects of photoinhibition and protein phosphorylation. Plant J **62:** 948–959

Goral TK, Johnson MP, Duffy CDP, Brain APR, Ruban AV, Mullineaux CW (2012) Light-harvesting antenna composition controls the macrostructure and dynamics of thylakoid membranes in Arabidopsis. Plant J **69:** 289–301

Green BR (2011) After the primary endosymbiosis: an update on the chromalveolate hypothesis and the origins of algae with Chl c. Photosynth Res **107:** 103–115

Johnson MP, Goral TK, Duffy CDP, Brain APR, Mullineaux CW, Ruban AV (2011) Photoprotective energy dissipation involves the reorganization of photosystem II light-harvesting complexes in the grana membranes of spinach chloroplasts. Plant Cell **23:** 1468–1479

Joshua S, Bailey S, Mann NH, Mullineaux CW (2005) Involvement of phycobilisome diffusion in energy quenching in cyanobacteria. Plant Physiol **138:** 1577–1585

Joshua S, Mullineaux CW (2004) Phycobilisome diffusion is required for light-state transitions in cyanobacteria. Plant Physiol **135:** 2112–2119

Joshua S, Mullineaux CW (2005) The rpaC gene product regulates phycobilisome-photosystem II interaction in cyanobacteria. Biochim Biophys Acta **1709:** 58–68

Kainz M, Lucotte M, Parrish CC (2002) Methyl mercury in zooplankton: the role of size, habitat, and food quality. Can J Fish Aquat Sci **59:** 1606–1615

Kaňa R (2013) Mobility of photosynthetic proteins. Photosynth Res **116:** 465–479

Kaňa R, Kotabová E, Komárek O, Šedivá B, Papageorgiou GC, Govindjee, Prášil O (2012a) The slow S to M fluorescence rise in cyanobacteria is due to a state 2 to state 1 transition. Biochim Biophys Acta **1817:** 1237–1247

Kaňa R, Kotabová E, Sobotka R, Prášil O (2012b) Non-photochemical quenching in cryptophyte alga Rhodomonas salina is located in chlorophyll a/c antennae. PLoS ONE **7:** e29700

Kaňa R, Matonoha C, Papáček S, Soukup J (2013) On estimation of diffusion coefficient based on spatio-temporal frap images: an inverse ill-posed problem. *In* J Chleboun, K Segeth, J Šístek, T Vejchodský eds, Programs and Algorithms of Numerical Mathematics 16. Institute of Mathematics, Academy of Sciences of the Czech Republic, Prague, pp 100–111.

Kaňa R, Prášil O, Komárek O, Papageorgiou GC, Govindjee (2009a) Spectral characteristic of fluorescence induction in a model cyanobacterium, Synechococcus sp. (PCC 7942). Biochim Biophys Acta **1787:** 1170–1178

Kaňa R, Prásil O, Mullineaux CW (2009b) Immobility of phycobilins in the thylakoid lumen of a cryptophyte suggests that protein diffusion in the lumen is very restricted. FEBS Lett **583:** 670–674

Khozin I, Adlerstein D, Bigongo C, Heimer YM, Cohen Z (1997) Elucidation of the biosynthesis of eicosapentaenoic acid in the microalga *Porphyridium cruentum*. II. Studies with radiolabeled precursors. Plant Physiol **114:** 223–230

Khozin-Goldberg I, Yu HZ, Adlerstein D, Didi-Cohen S, Heimer YM, Cohen Z (2000) Triacylglycerols of the red microalga Porphyridium cruentum can contribute to the biosynthesis of eukaryotic galactolipids. Lipids **35:** 881–889

Kirchhoff H (2007) Protein diffusion and macromolecular crowding in grana. Photosynth Res **91:** PS72

Kirchhoff H (2008a) Molecular crowding and order in photosynthetic membranes. Trends Plant Sci **13:** 201–207

Kirchhoff H (2008b) Significance of protein crowding, order and mobility for photosynthetic membrane functions. Biochem Soc Trans **36:** 967–970

Kirchhoff H (2014) Diffusion of molecules and macromolecules in thylakoid membranes. Biochim Biophys Acta **1837:** 495–502

Kirchhoff H, Haferkamp S, Allen JF, Epstein DBA, Mullineaux CW (2008) Protein diffusion and macromolecular crowding in thylakoid membranes. Plant Physiol **146:** 1571–1578

Kirchhoff H, Sharpe RM, Herbstova M, Yarbrough R, Edwards GE (2013) Differential mobility of pigment-protein complexes in granal and agranal thylakoid membranes of C_3 and C_4 plants. Plant Physiol **161:** 497–507

Kirilovsky D, Kaňa R, Prášil O (2014) Mechanisms modulating energy arriving at reaction centers in cyanobacteria. *In* B Demmig-Adams, W Adams, G Garab, Govindjee, eds, Non-Photochemical Quenching and Thermal Energy Dissipation In Plants, Algae and Cyanobacteria, Vol 40. Springer, Dordrecht, The Netherlands, in press

Koller KP, Wehrmeyer W, Schneider H (1977) Isolation and characterization of disc-shaped phycobilisomes from the red alga *Rhodella violacea*. Arch Microbiol **112:** 61–67

Kondo K, Ochiai Y, Katayama M, Ikeuchi M (2007) The membrane-associated CpcG2-phycobilisome in *Synechocystis*: a new photosystem I antenna. Plant Physiol **144:** 1200–1210

Kouřil R, Zygadlo A, Arteni AA, de Wit CD, Dekker JP, Jensen PE, Scheller HV, Boekema EJ (2005) Structural characterization of a complex of photosystem I and light-harvesting complex II of Arabidopsis thaliana. Biochemistry **44:** 10935–10940

Kowalczyk N, Rappaport F, Boyen C, Wollman FA, Collén J, Joliot P (2013) Photosynthesis in Chondrus crispus: the contribution of energy spill-over in the regulation of excitonic flux. Biochim Biophys Acta **1827:** 834–842

Krogmann DW, Pérez-Gómez B, Gutiérrez-Cirlos EB, Chagolla-López A, González de la Vara L, Gómez-Lojero C (2007) The presence of multidomain linkers determines the bundle-shape structure of the phycobilisome of the cyanobacterium Gloeobacter violaceus PCC 7421. Photosynth Res **93:** 27–43

Krupnik T, Kotabová E, van Bezouwen LS, Mazur R, Garstka M, Nixon PJ, Barber J, Kaňa R, Boekema EJ, Kargul J (2013) A reaction center-dependent photoprotection mechanism in a highly robust photosystem II from an extremophilic red alga, Cyanidioschyzon merolae. J Biol Chem **288:** 23529–23542

Lange W, Wilhelm C, Wehrmeyer W, Morschel E (1990) The supramolecular structure of photosystem II-phycobilisome complexes of Porphyridium cruentum. Bot Acta **103:** 250–257

Ley AC, Butler WL, Bryant DA, Glazer AN (1977) Isolation and function of allophycocyanin B of *Porphyridium cruentum*. Plant Physiol **59:** 974–980

Liberton M, Page LE, O'Dell WB, O'Neill H, Mamontov E, Urban VS, Pakrasi HB (2013) Organization and flexibility of cyanobacterial thylakoid membranes examined by neutron scattering. J Biol Chem **288:** 3632–3640

Lippincott-Schwartz J, Snapp E, Kenworthy A (2001) Studying protein dynamics in living cells. Nat Rev Mol Cell Biol **2:** 444–456

Liu H, Zhang H, Niedzwiedzki DM, Prado M, He G, Gross ML, Blankenship RE (2013) Phycobilisomes supply excitations to both photosystems in a megacomplex in cyanobacteria. Science **342:** 1104–1107

Liu LN, Aartsma TJ, Thomas JC, Lamers GEM, Zhou BC, Zhang YZ (2008a) Watching the native supramolecular architecture of photosynthetic membrane in red algae: topography of phycobilisomes and their crowding, diverse distribution patterns. J Biol Chem **283:** 34946–34953

Liu LN, Aartsma TJ, Thomas JC, Zhou BC, Zhang YZ (2009) FRAP analysis on red alga reveals the fluorescence recovery is ascribed to intrinsic photoprocesses of phycobilisomes than large-scale diffusion. PLoS ONE **4:** e5295

Liu LN, Bryan SJ, Huang F, Yu J, Nixon PJ, Rich PR, Mullineaux CW (2012) Control of electron transport routes through redox-regulated redistribution of respiratory complexes. Proc Natl Acad Sci USA **109:** 11431–11436

Liu LN, Chen XL, Zhang YZ, Zhou BC (2005) Characterization, structure and function of linker polypeptides in phycobilisomes of cyanobacteria and red algae: an overview. Biochim Biophys Acta **1708:** 133–142

Liu LN, Duquesne K, Oesterhelt F, Sturgis JN, Scheuring S (2011) Forces guiding assembly of light-harvesting complex 2 in native membranes. Proc Natl Acad Sci USA **108:** 9455–9459

Liu LN, Elmalk AT, Aartsma TJ, Thomas JC, Lamers GEM, Zhou BC, Zhang YZ (2008b) Light-induced energetic decoupling as a mechanism for phycobilisome-related energy dissipation in red algae: a single molecule study. PLoS ONE **3:** e3134

Lukšan L., Tůma M., Vlček J., Ramešová N., Šiška M., Hartman J., Matonoha C (2011) UFO 2011: Interactive System for Universal Functional Optimization. Institute of Computer Science, Czech Academy of Sciences, Prague, Technical Report No. 1151, p 305

Mareš J, Hrouzek P, Kaňa R, Ventura S, Strunecký O, Komárek J (2013) The primitive thylakoid-less cyanobacterium *Gloeobacter* is a common rock-dwelling organism. PLoS ONE **8:** e66323

Masood A, Stark KD, Salem N Jr (2005) A simplified and efficient method for the analysis of fatty acid methyl esters suitable for large clinical studies. J Lipid Res **46:** 2299–2305

McConnell MD, Koop R, Vasil'ev S, Bruce D (2002) Regulation of the distribution of chlorophyll and phycobilin-absorbed excitation energy in cyanobacteria: a structure-based model for the light state transition. Plant Physiol **130:** 1201–1212

Mika JT, Poolman B (2011) Macromolecule diffusion and confinement in prokaryotic cells. Curr Opin Biotechnol **22:** 117–126

Mimuro M, Kikuchi H (2003) Antenna systems and energy transfer in Cyanophyta and Rhodophyta. *In* BR Green, WW Parson, eds, Light-Harvesting Antennas in Photosynthesis, Vol 13. Springer, Dordrecht, The Netherlands, pp 281–306

Mullineaux CW (1992) Excitation energy transfer from phycobilisomes to photosystem I in a cyanobacterium. Biochim Biophys Acta **1100:** 285–292

Mullineaux CW (1994) Excitation energy transfer from phycobilisomes to photosystem I in a cyanobacterial mutant lacking photosystem II. Biochim Biophys Acta **1184:** 71–77

Mullineaux CW (2008a) Factors controlling the mobility of photosynthetic proteins. Photochem Photobiol **84:** 1310–1316

Mullineaux CW (2008b) Phycobilisome-reaction centre interaction in cyanobacteria. Photosynth Res **95:** 175–182

Mullineaux CW, Bittersmann E, Allen JF, Holzwarth AR (1990) Picosecond time-resolved fluorescence emission spectra indicate decreased energy transfer from the phycobilisome to photosystem II in light state 2 in the cyanobacterium Synechococcus. Biochim Biophys Acta **1015:** 231–242

Mullineaux CW, Tobin MJ, Jones GR (1997) Mobility of photosynthetic complexes in thylakoid membranes. Nature **390:** 421–424

Nagy G, Szabó M, Unnep R, Káli G, Miloslavina Y, Lambrev PH, Zsiros O, Porcar L, Timmins P, Rosta L, et al (2012) Modulation of the multilamellar membrane organization and of the chiral macrodomains in the diatom Phaeodactylum tricornutum revealed by small-angle neutron scattering and circular dichroism spectroscopy. Photosynth Res **111:** 71–79

Neilson JAD, Durnford DG (2010) Structural and functional diversification of the light-harvesting complexes in photosynthetic eukaryotes. Photosynth Res **106:** 57–71

Papáček Š, Kaňa R, Matonoha C (2013) Estimation of diffusivity of phycobilisomes on thylakoid membrane based on spatio-temporal FRAP images. Math Comput Model **57:** 1907–1912

Papageorgiou GC, Tsimilli-Michael M, Stamatakis K (2007) The fast and slow kinetics of chlorophyll a fluorescence induction in plants, algae and cyanobacteria: a viewpoint. Photosynthesis Research **94:** 275–290

Phair RD, Gorski SA, Misteli T (2004) Measurement of dynamic protein binding to chromatin in vivo, using photobleaching microscopy. Chromatin and Chromatin Remodeling Enzymes Part A **375:** 393–414

Rakhimberdieva MG, Boichenko VA, Karapetyan NV, Stadnichuk IN (2001) Interaction of phycobilisomes with photosystem II dimers and photosystem I monomers and trimers in the cyanobacterium Spirulina platensis. Biochemistry **40:** 15780–15788

Sarcina M, Mullineaux CW (2004) Mobility of the IsiA chlorophyll-binding protein in cyanobacterial thylakoid membranes. J Biol Chem **279:** 36514–36518

Sarcina M, Tobin MJ, Mullineaux CW (2001) Diffusion of phycobilisomes on the thylakoid membranes of the cyanobacterium Synechococcus 7942: effects of phycobilisome size, temperature, and membrane lipid composition. J Biol Chem **276:** 46830–46834

Stadnichuk IN, Bulychev AA, Lukashev EP, Sinetova MP, Khristin MS, Johnson MP, Ruban AV (2011) Far-red light-regulated efficient energy transfer from phycobilisomes to photosystem I in the red microalga Galdieria sulphuraria and photosystems-related heterogeneity of phycobilisome population. Biochim Biophys Acta **1807:** 227–235

Su HN, Xie BB, Zhang XY, Zhou BC, Zhang YZ (2010) The supramolecular architecture, function, and regulation of thylakoid membranes in red algae: an overview. Photosynth Res **106:** 73–87

Tamary E, Kiss V, Nevo R, Adam Z, Bernát G, Rexroth S, Rögner M, Reich Z (2012) Structural and functional alterations of cyanobacterial phycobilisomes induced by high-light stress. Biochim Biophys Acta **1817:** 319–327

Thangaraj B, Jolley CC, Sarrou I, Bultema JB, Greyslak J, Whitelegge JP, Lin S, Kouřil R, Subramanyam R, Boekema EJ, et al (2011) Efficient light harvesting in a dark, hot, acidic environment: the structure and function of PSI-LHCI from Galdieria sulphuraria. Biophys J **100:** 135–143

Theiss C, Schmitt FJ, Pieper J, Nganou C, Grehn M, Vitali M, Olliges R, Eichler HJ, Eckert HJ (2011) Excitation energy transfer in intact cells and in the phycobiliprotein antennae of the chlorophyll d containing cyanobacterium Acaryochloris marina. J Plant Physiol **168:** 1473–1487

Tsekos I, Reiss HD, Delivopoulos SG (2004) The supramolecular organization of photosynthetic membranes in the red alga Thorea ramosissima: spatial relationship between putative photosystem II core particles (EF-particles) and phycobilisomes. Phycologia **43:** 543–551

Vanselow C, Weber APM, Krause K, Fromme P (2009) Genetic analysis of the photosystem I subunits from the red alga, Galdieria sulphuraria. Biochim Biophys Acta **1787:** 46–59

Wang L, Mao Y, Kong F, Li G, Ma F, Zhang B, Sun P, Bi G, Zhang F, Xue H, et al (2013) Complete sequence and analysis of plastid genomes of two economically important red algae: Pyropia haitanensis and Pyropia yezoensis. PLoS ONE **8:** e65902

Wolfe GR, Cunningham FX, Durnford D, Green BR, Gantt E (1994) Evidence for a common origin of chloroplasts with light-harvesting complexes of different pigmentation. Nature **367:** 566–568

Yokono M, Murakami A, Akimoto S (2011) Excitation energy transfer between photosystem II and photosystem I in red algae: larger amounts of phycobilisome enhance spillover. Biochim Biophys Acta **1807:** 847–853

Yoon HS, Muller KM, Sheath RG, Ott FD, Bhattacharya D (2006) Defining the major lineages of red algae (Rhodophyta). J Phycol **42:** 482–492